Supporting Information

Synergistic Effect of Ti^{3+} Doping and Facet Regulation over Ti^{3+} Doped TiO_2 Nanosheets with Enhanced Photoreactivity

Xiaogang Liu[a*] and Yingpu Bi[b*]

[a] *College of Chemistry and Chemical Engineering, Xinyang Normal University, Xinyang 464000, China. Email: lxg133298@163.com.*

[b] *State Key Laboratory for Oxo Synthesis & Selective Oxidation, National Engineering Research Center for Fine Petrochemical Intermediates, Lanzhou Institute of Chemical Physics, CAS, Lanzhou 730000, China. E-mail: yingpubi@licp.cas.cn.*

Additional figures

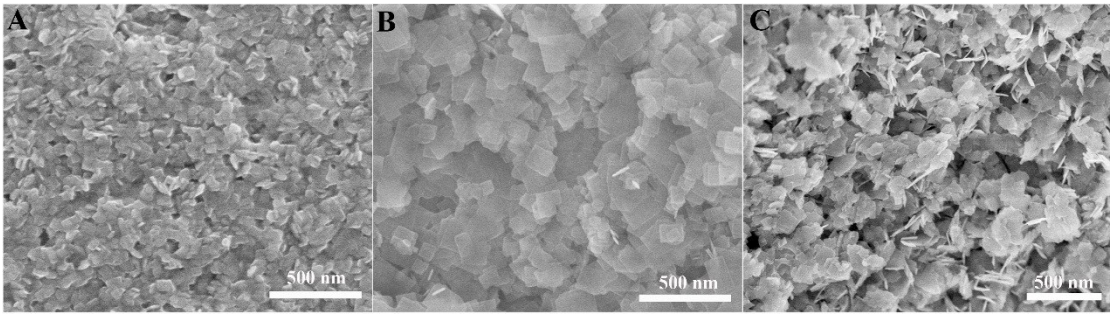

Fig.S1 SEM images of Air-TiO_2-HF4.5 (A), Air-TiO_2-HF6 (B) and Air-TiO_2-HF9(C).

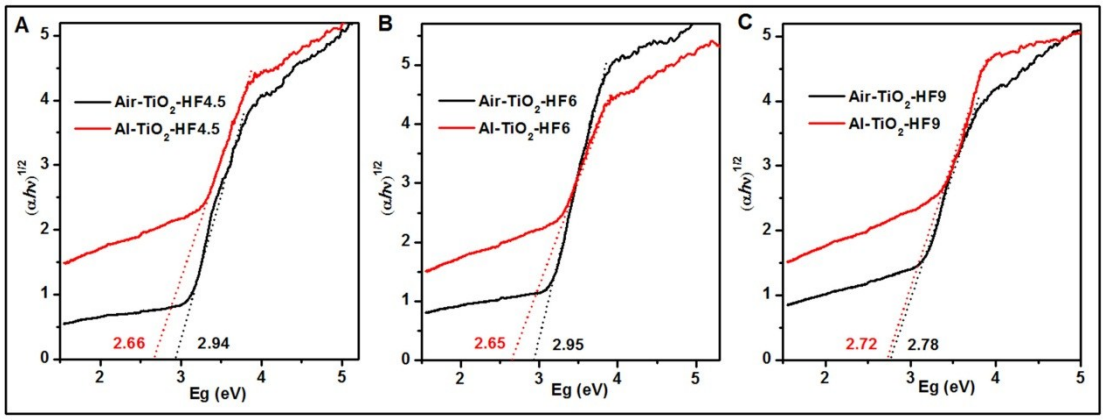

Fig. S2 Curves of the Kubelka–Munk function plotted against the photon energy for the samples before (black line) and after (red line) Al reduction with different volume of HF: A) 4.5 mL, B) 6 mL, and C) 9 mL.

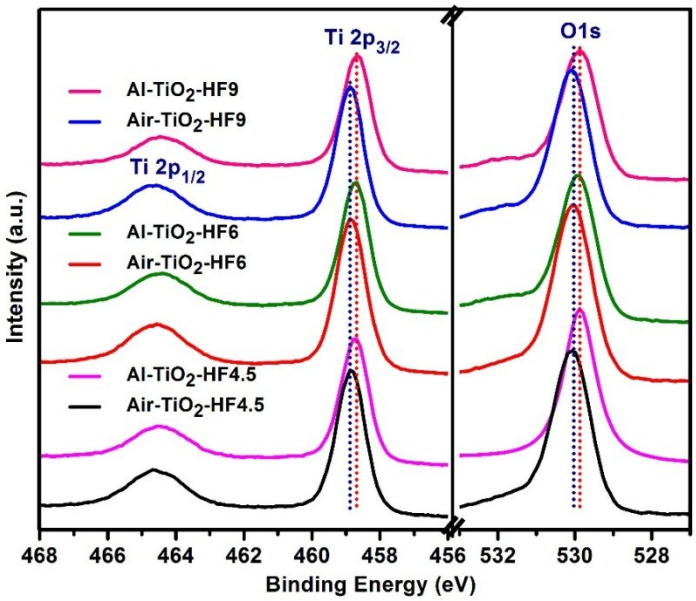

Fig. S3 High resolution XPS spectra of Ti 2p and O 1s XPS spectra of TiO_2 nanosheets treated before and after Al reduction.

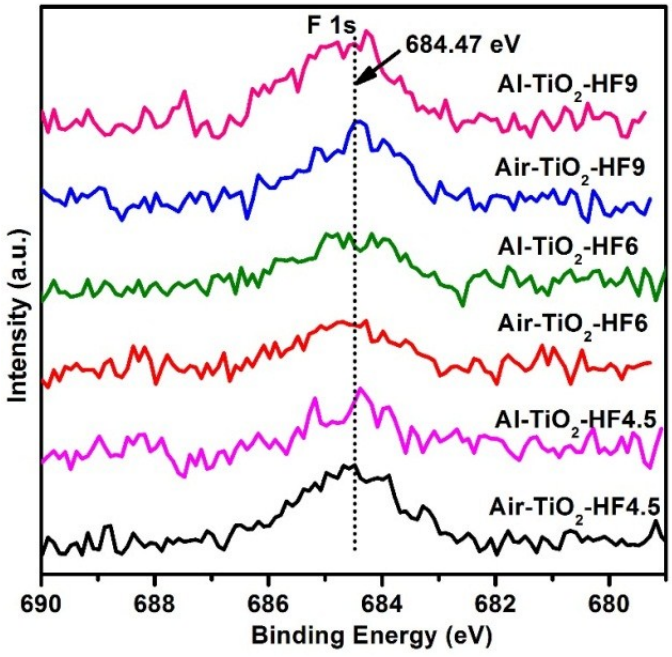

Fig. S4 (A) F 1s XPS spectra of pristine TiO_2 and Al reduced TiO_2

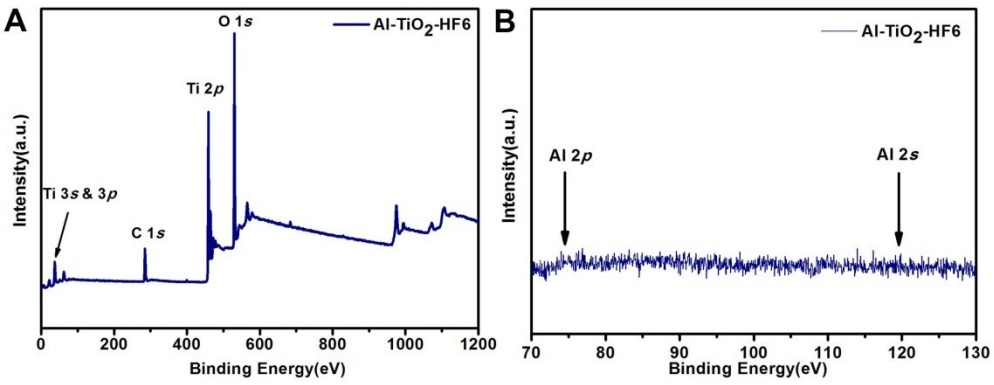

Fig. S5 XPS survey spectra and Al element analysis of of Al-TiO_2-HF6 sample.

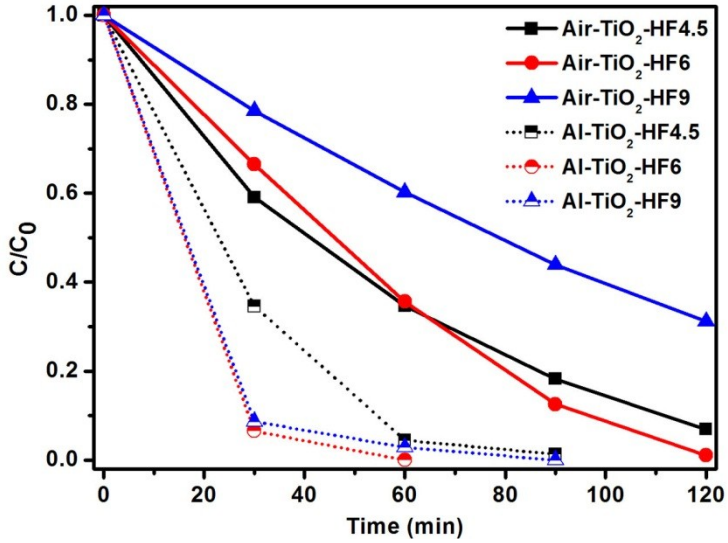

Fig. S6 UV-vis light induced photocatalytic degradation of methylene orange of as prepared TiO_2 nanosheets treated before and after Al reduction.

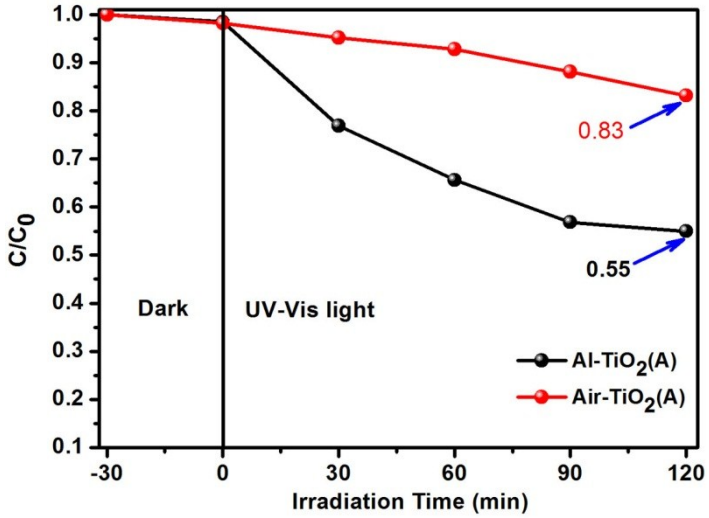

Fig. S7 UV-vis light induced photocatalytic degradation of methylene orange of Al-TiO_2 (A) and Air-TiO_2 (A) samples.

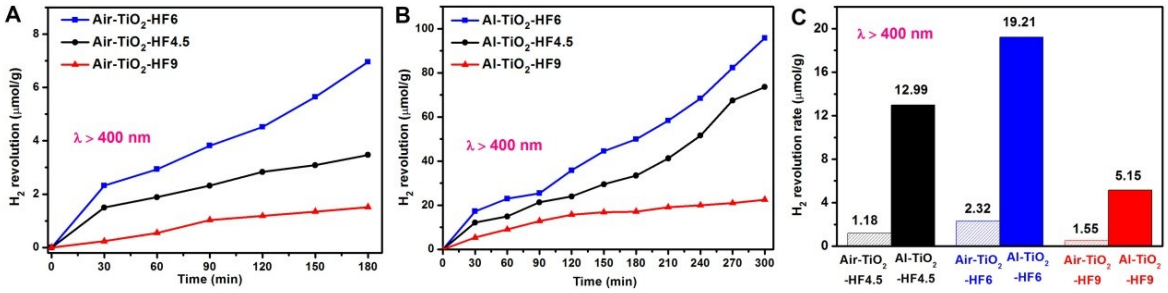

Fig. S8 Photocatalytic H_2 evolution over TiO_2 treated (A) before and (B) after Al reduction and their comparative study of H_2 evolution rates (C) under visible light irradiation (λ>400 nm)

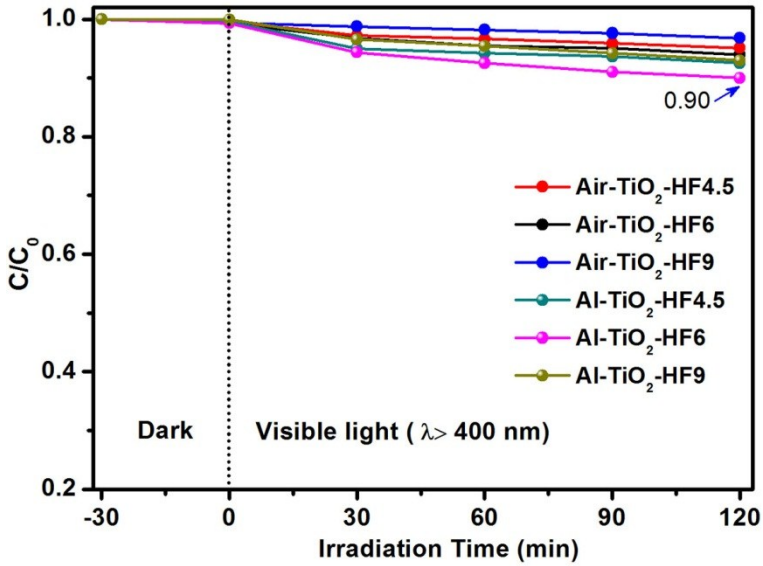

Fig. S9 Visible light ((λ>400 nm)) induced photocatalytic degradation of methylene orange of as prepared TiO_2 nanosheets treated before and after Al reduction.

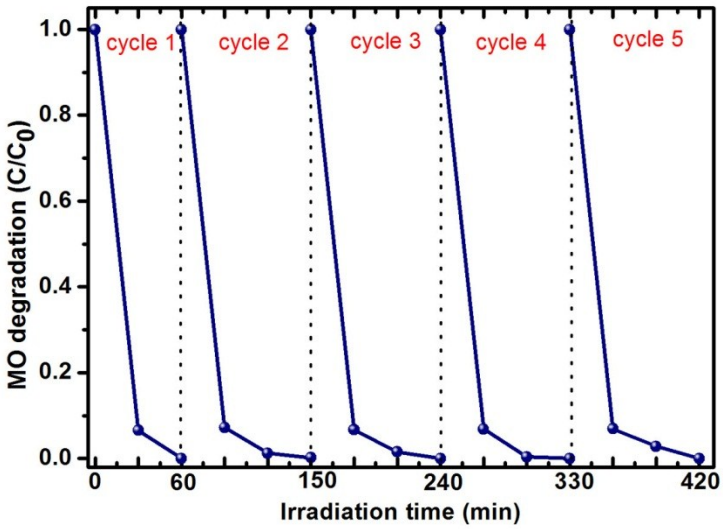

Fig.S10 Stability tests of UV-vis light irradiation induced photocatalytic activities (MO decomposition) of the as prepared Al-TiO_2-HF6 nanosheets.

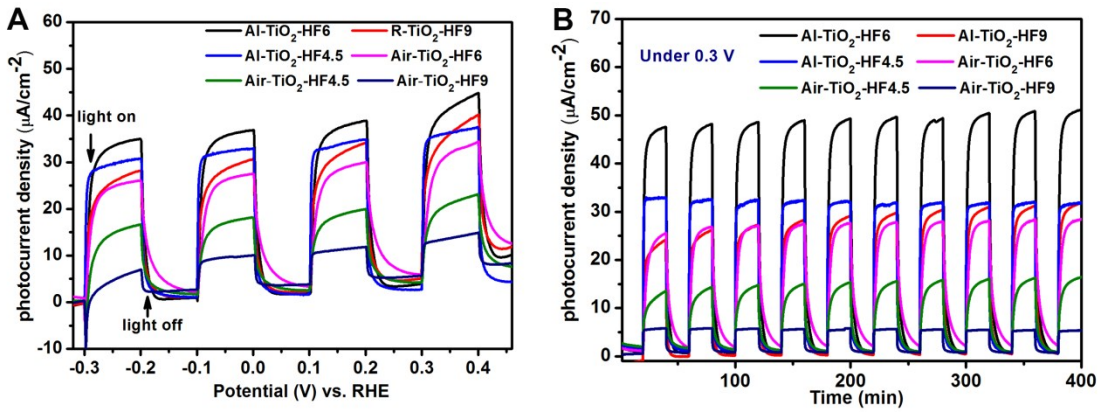

Fig. S11 Photoelectrochemical properties of pristine TiO_2 and Al-reduced TiO_2 electrodes: (A) chopped *J–V* curves and (B) *I–t* amperometric curves under UV-Vis light illumination using a three electrode setup (TiO_2 working, Pt counter, saturated calomel reference electrode) in a 1 M NaOH electrolyte.

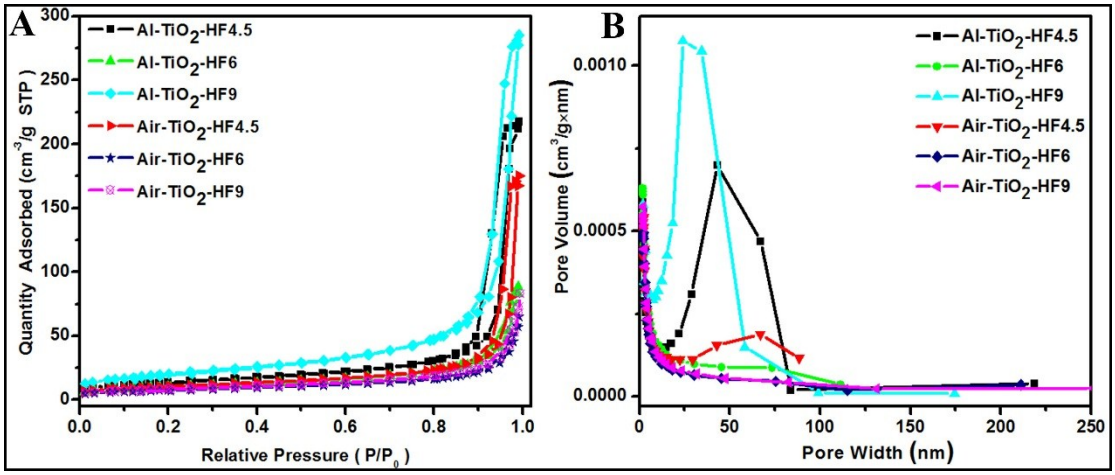

Fig. S12 N_2 adsorption-desorption isotherm (A) and pore size distribution (B) of prepared TiO_2 nanosheets samples before and after Al reduction.

Table S1. Structural information of as-synthesized Al reduced TiO_2 nanosheets synthesized at different reaction conditions.

sample	Average Thickness (nm)	Average Length (nm)	Percentage of {001} Facet
Al-TiO_2-HF4.5	7.2	40-50	58
Al-TiO_2-HF6	5.9	120-150	72
Al-TiO_2-HF9	5.1	50-60	83

Table S2. Structure information of BET specific surface areas, average pore width and total pore volume for as prepared TiO_2 samples before and after Al reduction

Sample	BET specific surface areas (m^2/g)	Average pore width (nm)	Total pore volume (cm^3/g)
Air-TiO_2-HF4.5	37.48	8.95	0.083895
Al-TiO_2-HF4.5	49.86	22.42	0.279436
Air-TiO_2-HF6	73.86	15.12	0.279157
Al-TiO_2-HF6	26.45	8.42	0.05783
Air-TiO_2-HF9	29.39	8.62	0.066025
Al-TiO_2-HF9	39.61	10.89	0.103493